

# Molecular structure of a hyperactive antifreeze protein adsorbed to ice F

Cite as: J. Chem. Phys. **150**, 131101 (2019); <https://doi.org/10.1063/1.5090589>

Submitted: 29 January 2019 . Accepted: 01 March 2019 . Published Online: 02 April 2019

K. Meister , C. J. Moll, S. Chakraborty, B. Jana, A. L. DeVries, H. Ramløv, and H. J. Bakker 

## COLLECTIONS

F This paper was selected as Featured



View Online



Export Citation



CrossMark

## ARTICLES YOU MAY BE INTERESTED IN

### Ions' motion in water

The Journal of Chemical Physics **150**, 190901 (2019); <https://doi.org/10.1063/1.5090765>

### Advances in the experimental exploration of water's phase diagram

The Journal of Chemical Physics **150**, 060901 (2019); <https://doi.org/10.1063/1.5085163>

### Unsupervised machine learning in atomistic simulations, between predictions and understanding

The Journal of Chemical Physics **150**, 150901 (2019); <https://doi.org/10.1063/1.5091842>

## Lock-in Amplifiers up to 600 MHz

starting at

\$6,210



 Zurich  
Instruments

Watch the Video 



# Molecular structure of a hyperactive antifreeze protein adsorbed to ice

Cite as: J. Chem. Phys. 150, 131101 (2019); doi: 10.1063/1.5090589

Submitted: 29 January 2019 • Accepted: 1 March 2019 •

Published Online: 2 April 2019



View Online



Export Citation



CrossMark

K. Meister,<sup>1</sup>  C. J. Moll,<sup>2</sup> S. Chakraborty,<sup>3</sup> B. Jana,<sup>3</sup> A. L. DeVries,<sup>4</sup> H. Ramløv,<sup>5</sup> and H. J. Bakker<sup>2</sup> 

## AFFILIATIONS

<sup>1</sup>Max Planck Institute for Polymer Science, 55128 Mainz, Germany

<sup>2</sup>AMOLF, Science Park 104, 1098 XG Amsterdam, The Netherlands

<sup>3</sup>Department of Physical Chemistry, Indian Association for the Cultivation of Science, Kolkata, India

<sup>4</sup>Department of Animal Biology, University of Illinois at Urbana–Champaign, Urbana, Illinois 61801, USA

<sup>5</sup>Department of Science and Environment, Roskilde University, 4000 Roskilde, Denmark

## ABSTRACT

Antifreeze proteins (AFPs) are a unique class of proteins that bind to ice crystal surfaces and arrest their growth. The working mechanism of AFPs is not well understood because, as of yet, it was not possible to perform molecular-scale studies of AFPs adsorbed to the surface of ice. Here, we study the structural properties of an AFP from the insect *Rhagium mordax* (*RmAFP*) adsorbed to ice with surface specific heterodyne-detected vibrational sum-frequency generation spectroscopy and molecular dynamic simulations. We find that *RmAFP*, unlike other proteins, retains its hydrating water molecules upon adsorption to the ice surface. This hydration water has an orientation and hydrogen-bond structure different from the ice surface, thereby inhibiting the insertion of water layers in between the protein and the ice surface.

Published under license by AIP Publishing. <https://doi.org/10.1063/1.5090589>

Cold-adapted ectotherms living at subzero temperatures have evolved an elegant macromolecular solution to deal with the lethal threat of ice formation in their tissues. They produce antifreeze proteins (AFPs) that depress the freezing point of water in a noncolligative manner.<sup>1</sup> They are of great interest for their use in antifreeze formulations for frozen food,<sup>2</sup> waterborne paints,<sup>3</sup> cryopreservation,<sup>4</sup> and other water-based materials.<sup>5</sup> The molecular details of the working mechanism of AFPs are poorly understood, which is mostly due to the fact that experimental studies of AFP-ice complexes are difficult.<sup>6</sup> Recent studies involving ice etching and the analysis of ice crystal growth morphology changes provided information on the ice plane specificities of AFPs,<sup>7,8</sup> but did not reveal the molecular-scale mechanisms by which AFPs bind to ice and by which they inhibit ice crystal growth. In particular, information on the ice surface, adsorbed AFPs, and the surrounding water would be of great value, as several simulation studies suggest a critical role of the hydration layers in the recognition and binding of AFPs to ice.<sup>9–12</sup>

Here, we use heterodyne-detected vibrational sum-frequency generation (HD-VSFG) spectroscopy to study AFP of *Rhagium mordax* (*RmAFP*) adsorbed to a monocrystalline, basal ice surface.<sup>13</sup> We

measure the real (Re) and imaginary (Im) part of the second-order susceptibility  $\chi^{(2)}$  of the vibrations at the surface, which provides direct information on the absolute orientation of the surface-bound molecules.<sup>14</sup> *RmAFP* is the most active AFP known and can bind to the basal and prism ice face. It is part of a large group of AFPs that possess an array of ordered threonine residues on a flat  $\beta$ -sheet region at their ice-binding site (Fig. S1).<sup>15–18</sup>

In Figs. 1(a)–1(d), we present  $\text{Im}[\chi^{(2)}]$  spectra of  $\alpha$ -lactalbumin,  $\beta$ -lactoglobulin, myoglobin, and *RmAFP* at the surfaces of water and ice. At the surface of water, the HD-VSFG spectra of the non-AFP and *RmAFP* solutions look very similar. All spectra show contributions from aliphatic C–H stretch vibrations ( $\sim 2880\text{ cm}^{-1}$  and  $\sim 2930\text{ cm}^{-1}$ ) and aromatic ( $\sim 3060\text{ cm}^{-1}$ ) C–H vibrations of the amino acid residues of the proteins. At frequencies  $>3100\text{ cm}^{-1}$ , all spectra show a broad positive band that we assign to the O–H stretching vibrations of interfacial water molecules. The sign of  $\text{Im}[\chi^{(2)}]$  is determined by the orientation of the vibrational transition dipole moment. In the case of well-defined local modes, the orientation of the transition dipole moment of a vibration can be directly related to the orientation of the molecular group carrying that vibration. For liquid water and ice, the O–H stretch vibrations

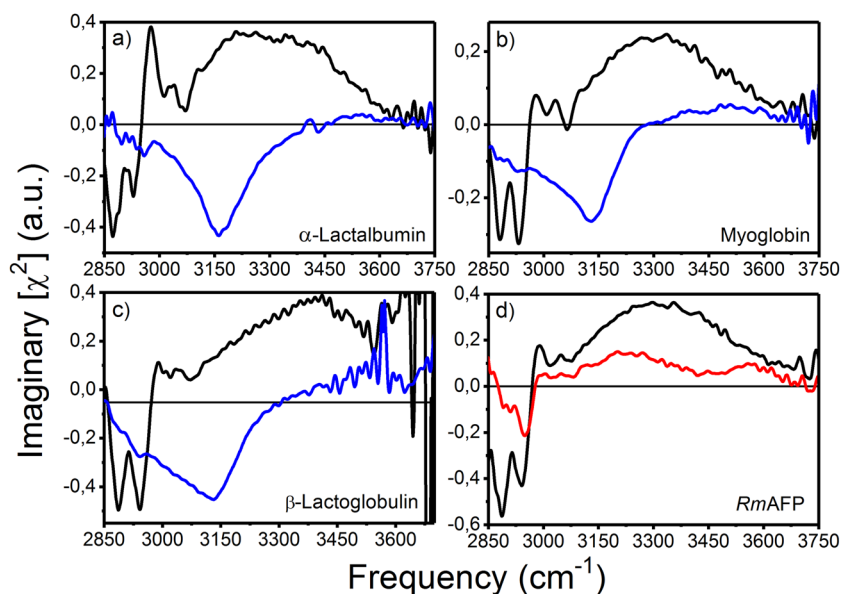


**FIG. 1.** Imaginary  $[\chi^{(2)}]$  spectra of  $15 \mu\text{M}$  solutions of  $\alpha$ -lactalbumin (a), myoglobin (b),  $\beta$ -lactoglobulin (c), and *RmAFP* (d) ( $20 \text{ mM NaPo}_4$ ,  $150 \text{ mM NaCl}$ , and  $\text{pH } 7.0$ ) at the solution-air interface and deposited on the basal face of monocrystalline ice. The HD-VSFG spectra of the aqueous protein solutions (black) look similar with characteristic C–H and O–H stretch vibrations. Deposition of non-AFP solutions (a)–(c) on the surface of ice results in spectra with a dominant negative peak at  $\sim 3150 \text{ cm}^{-1}$ . With identical conditions, the deposition of an *RmAFP* solution shows a very different imaginary  $[\chi^{(2)}]$  spectrum with a positive band centered at  $\sim 3200 \text{ cm}^{-1}$ . The measurements at the water surface (black) were performed at  $293 \text{ K}$ , and those of the ice surface were performed at  $255 \text{ K}$  and with the SSP polarization configuration (s-SFG, s-VIS, p-IR).

are delocalized and thus the relation between the sign of  $\text{Im}[\chi^{(2)}]$  and the orientation of the individual molecules is less straightforward. In this case, the sign of  $\text{Im}[\chi^{(2)}]$  is determined by the dominant orientation of the transition dipole moments of the delocalized O–H stretch vibrations. A positive sign indicates that there are more delocalized O–H stretch vibrations involving O–H groups for which the hydrogen atoms are pointing towards the air (up), while a negative sign of  $\text{Im}[\chi^{(2)}]$  indicates that there are more delocalized O–H vibrations involving O–H groups for which the hydrogen atoms are pointing into the liquid (down). Hence, although for liquid water and ice  $\text{Im}[\chi^{(2)}]$  cannot directly be related to particular hydrogen-bonded O–H groups, a positive sign of  $\text{Im}[\chi^{(2)}]$  still implies that the interfacial water molecules have a preferential orientation with their O–H groups pointing to the negatively charged proteins floating on the water surface.<sup>19–21</sup>

The broad shape of the O–H band observed for *RmAFP* on water indicates that the protein does not possess a pre-ordered hydration layer. Such a pre-ordered water layer has been observed experimentally for AFP III.<sup>22</sup> The absence of a pre-ordered hydration layer for *RmAFP* agrees with the results of recent molecular dynamics simulations.<sup>11</sup>

For  $\alpha$ -lactalbumin,  $\beta$ -lactoglobulin, myoglobin, and *RmAFP* adsorbed to the ice surface the  $\text{Im}[\chi^{(2)}]$  spectra again show the responses of the C–H stretch vibrations of the proteins. For the non-AFPs, the  $\text{Im}[\chi^{(2)}]$  spectra are dominated by a strong negative band centered at  $\sim 3150 \text{ cm}^{-1}$  that is similar to the signal that is observed at the bare ice-air interface (Fig. S2). This band has been assigned to the bilayer-stitching O–H stretch vibrations of the water molecules in the top two bilayers of the ice crystal.<sup>13,23</sup> The negative sign indicates that these water molecules have a net orientation with their O–H groups pointing away from the surface. This result shows that for non-AFPs, the hydrogen-bond structure and orientation of water molecules at and near the interface are completely determined by the mutual interactions of water molecules in ice.

The  $\text{Im}[\chi^{(2)}]$  spectrum of *RmAFP* at the surface of ice shows a positive signal centered at  $\sim 3200 \text{ cm}^{-1}$ . This result shows that *RmAFP* remains hydrated with water molecules with an orientation that is determined by the *RmAFP*, even after adsorption of the protein to the ice surface. The spectral shape of the hydration water signal changes somewhat upon adsorption to the ice surface. We observe a shift in the center frequency from  $\sim 3300 \text{ cm}^{-1}$  at temperatures above the melting point to  $\sim 3200 \text{ cm}^{-1}$  at temperatures below the melting point, which indicates that the water molecules in the hydration layer of *RmAFP* become more strongly hydrogen-bonded upon adsorption of the protein to ice. The spectrum is broader and blueshifted compared to that of ice, showing that the hydrogen-bond structure of the hydration layer differs from that of ice. We further observe resonances at  $\sim 2880 \text{ cm}^{-1}$ ,  $\sim 2930 \text{ cm}^{-1}$ , and  $3060 \text{ cm}^{-1}$  that we assign to C–H vibrations of the protein and a signal at  $\sim 3560 \text{ cm}^{-1}$  that we assign to crystalline ice.<sup>13</sup>

We explain the persistent presence of hydrating water molecules for *RmAFP* from the rigid, corrugated structure of the ice-binding surface (IBS) of *RmAFP*. The IBS consists of ridges with a high density of threonine residues that strongly interact with the surface of ice. Such a corrugated motif of the IBS is common for insect and other hyperactive antifreeze proteins.<sup>11</sup>

In a previous study on the related hyperactive antifreeze protein from the beetle *Dendroides canadensis* (DAFP-1) at the water surface, we showed that the valleys between these ridges contain hydrating water molecules.<sup>24</sup> Such “channel water molecules” were also observed in crystal structures and simulations of related AFPs.<sup>11,17,18</sup> The present results indicate that the corrugated structure of *RmAFP* with ridges and valleys containing hydration water persists when the protein adsorbs to ice.

Most other non-AFPs, including the proteins used in this study, do not possess such a rigid, corrugated surface and will likely unfold and stretch out on the ice surface. As a result, for these proteins, no

protein-oriented water molecules in between the ice surface and the protein are observed.

To corroborate the above explanation, we performed molecular dynamics simulations of the adsorption of *RmAFP* and  $\alpha$ -lactalbumin to the surface of ice using Groningen Machine for Chemical Simulations 4.5 (GROMACS 4.5). We find that for  $\alpha$ -lactalbumin, a large fraction of the amino-acid residues are in

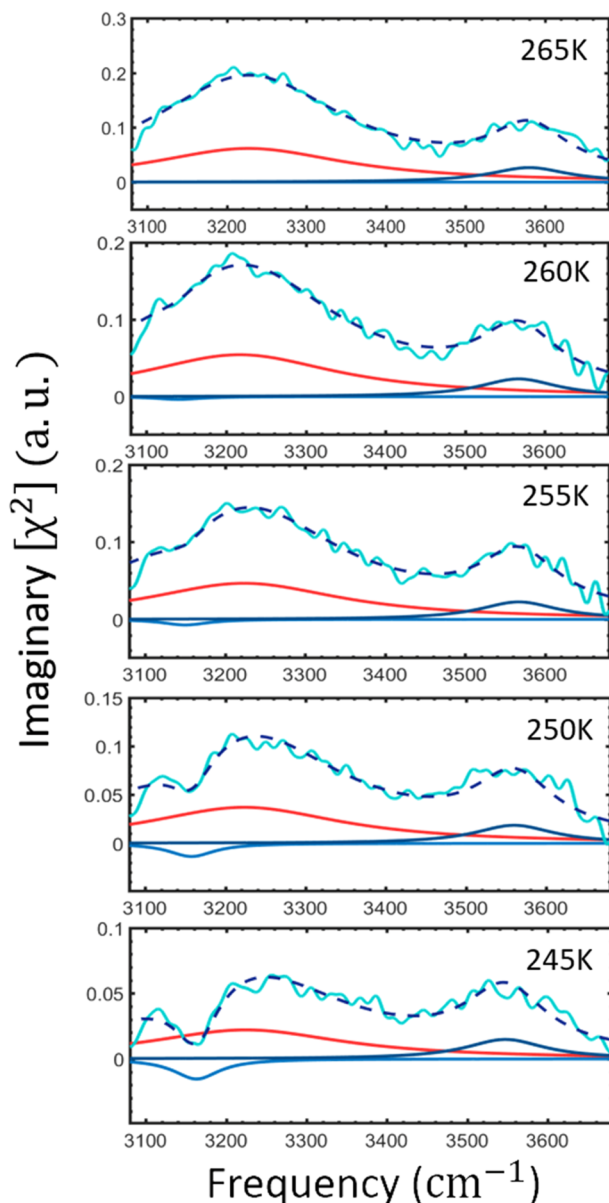


**FIG. 2.** Imaginary  $[\chi^2]$  spectra of *RmAFP* at the surface of basal ice at temperatures between 245 and 265 K. The spectra are fitted with three Lorentzian bands (solid red, light blue, and blue lines). The measured data are represented by the cyan line, and the fitted spectra by dashed black lines. Decreasing the temperature leads to a decrease of the  $\sim 3200\text{ cm}^{-1}$  signal and to an ingrowth of a signal at  $\sim 3180\text{ cm}^{-1}$ .

direct contact with the ice surface, whereas for *RmAFP*, the interfacial region contains water molecules that hydrate the protein and are not associated with those in the ice crystal (Figs. S3 and S4). These water domains between the IBS of the adsorbed *RmAFP* and the ice surface have a tetrahedrally coordinated arrangement, which is in excellent agreement with the observed center frequency of  $3200\text{ cm}^{-1}$  in the  $\text{Im}[\chi^2]$  spectrum of *RmAFP* adsorbed to ice.

In Fig. 2, we show  $\text{Im}[\chi^2]$  spectra of *RmAFP* at the ice surface at different temperatures in the range between 265 K and 245 K. We find that the signals at  $\sim 3200\text{ cm}^{-1}$  and  $\sim 3560\text{ cm}^{-1}$  decrease when the temperature is lowered. We also observe an ingrowth of a negative band at  $\sim 3180\text{ cm}^{-1}$  that we assign to the O–H vibrations of crystalline ice. We performed a spectral decomposition of the  $\text{Im}[\chi^2]$  spectra to obtain quantitative information on the temperature dependence of the hydration-shell band and the ice band. In Fig. 3, we plot the areas of these bands as a function of temperature. We explain the observed temperature dependence of the band areas from the change in orientation and binding of the water molecules between the IBS of the adsorbed *RmAFP* and the ice surface. Decreasing the temperature causes the water domains to reorient away from the AFP and to join the ice lattice, thereby lowering the signal at  $\sim 3200\text{ cm}^{-1}$ . The newly formed ice layers of the *RmAFP* solution give rise to the negative signal at  $\sim 3180\text{ cm}^{-1}$ .

The functioning of AFPs is intimately connected to the mechanism by which these proteins bind to ice and how they prevent further growth of the ice crystal at and near their adsorption sites. All AFPs are proposed to function according to the adsorption-inhibition mechanism.<sup>25</sup> In this mechanism, ice can only grow in between the adsorbed AFPs, which results in a strongly curved ice surface with a high associated surface energy.<sup>25</sup> This so-called Kelvin effect explains the depression of the freezing point. We speculate that the different orientation and hydrogen-bond structure of the water molecules in the valleys between the ridges of the IBS will inhibit the intercalation of ice layers in between the adsorbed hyperactive AFP and the ice surface. As a result, the adsorbed hyperactive AFPs are

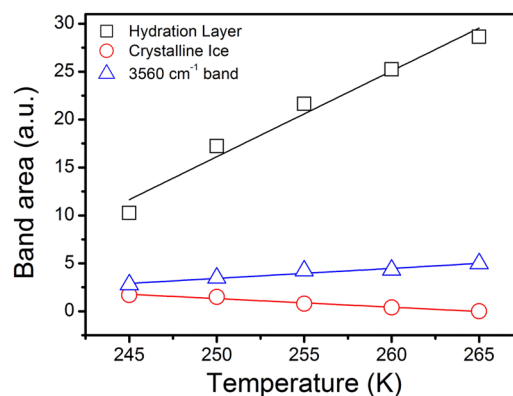


**FIG. 3.** Areas of the three different bands used in the spectral decomposition of the temperature-dependent imaginary  $[\chi^2]$  spectra of Fig. 2. The bands are assigned to crystalline ice signal at  $3180\text{ cm}^{-1}$  (red circles), the hydration shell of *RmAFP* at  $3200\text{ cm}^{-1}$  (black squares), and a weaker crystalline ice signal at  $3560\text{ cm}^{-1}$  (blue triangles). The lines serve as guides to the eye.

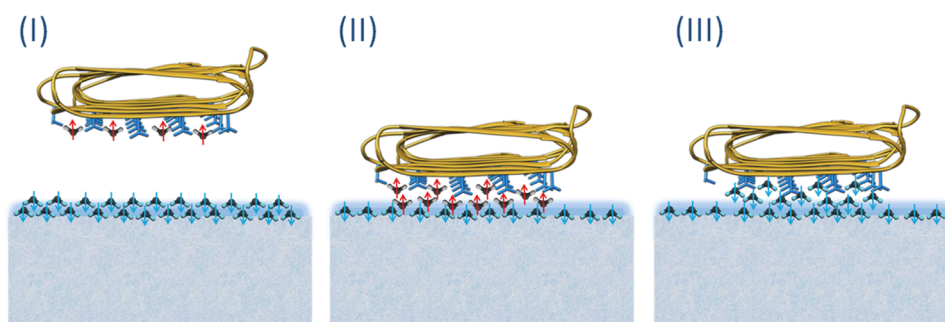


**FIG. 4.** Schematic representation of the ice-binding and ice-crystal growth inhibition mechanism of AFPs. The ice surface contains a water layer, in which the water molecules have a net orientation with their O–H groups pointing towards the ice. (I) *RmAFP* has water molecules in the valleys of the IBS that have an orientation towards the protein. (II) *RmAFP* accumulates at the interfacial region of ice and retains its hydrating water molecules at the IBS of which the orientation is determined by the protein and not by the ice surface. (III) Water molecules cannot intercalate between the hydration water and the surface, so that ice can only grow in between adsorbed AFPs, which results in a strongly curved ice surface with a high associated surface energy.

not pushed away from the original ice surface, and ice can only grow in between the adsorbed *RmAFP*s, leading to a pronounced Kelvin effect. Hence, the water molecules between the ridges of the IBS of *RmAFP* are needed for the antifreeze mechanism of *RmAFP* and other hyperactive AFPs. The mechanism of adsorption of *RmAFP* to ice is schematically shown in Fig. 4.

See [supplementary material](#) for the experimental setup, experimental methods, simulation methods, and Figs. S1–S4.

This work was part of the research program of the Netherlands Organization for Scientific Research (NWO) and was performed at the research institute AMOLF. B.J. acknowledges financial support from the Department of Science and Technology (India) SERB (Grant No. EMR/2016/001333). The authors acknowledge the central supercomputing facility (CRAY) at Indian Association for the Cultivation of Science, Kolkata, India.

## REFERENCES

- <sup>1</sup>A. L. DeVries, *Science* **172**, 1152 (1971).
- <sup>2</sup>M. Hassas-Roudsari and H. D. Goff, *Food Res. Int.* **46**, 425 (2012).
- <sup>3</sup>A. P. Esser-Kahn, V. Trang, and M. B. Francis, *J. Am. Chem. Soc.* **132**, 13264 (2010).
- <sup>4</sup>G. Amir, L. Horowitz, B. Rubinsky, B. S. Yousif, J. Lavee, and A. K. Smolinsky, *Cryobiology* **48**, 273 (2004).
- <sup>5</sup>H. J. Kim, J. H. Lee, Y. B. Hur, C. W. Lee, S. H. Park, and B. W. Koo, *Mar. Drugs* **15**, 27 (2017).
- <sup>6</sup>K. A. Sharp, *Proc. Natl. Acad. Sci. U. S. A.* **108**, 7281 (2011).
- <sup>7</sup>C. A. Knight, C. C. Cheng, and A. L. DeVries, *Biophys. J.* **59**, 409 (1991).
- <sup>8</sup>M. Bar, Y. Celik, D. Fass, and I. Braslavsky, *Cryst. Growth Des.* **8**, 2954 (2008).
- <sup>9</sup>M. J. Kuiper, C. J. Morton, S. E. Abraham, and A. Gray-Weale, *eLife* **4**, e05142 (2015).
- <sup>10</sup>S. Chakraborty and B. Jana, *Langmuir* **33**, 7202 (2017).
- <sup>11</sup>A. Hudait, N. Odendahl, Y. Qiu, F. Paesani, and V. Molinero, *J. Am. Chem. Soc.* **140**, 4905 (2018).
- <sup>12</sup>D. R. Nutt and J. C. Smith, *J. Am. Chem. Soc.* **130**, 13066 (2008).
- <sup>13</sup>W. J. Smit, F. Tang, Y. Nagata, M. A. Sánchez, T. Hasegawa, E. H. G. Backus, M. Bonn, and H. J. Bakker, *J. Phys. Chem. Lett.* **8**, 3656 (2017).
- <sup>14</sup>Y. R. Shen, *Nature* **337**, 519 (1989).
- <sup>15</sup>E. Kristiansen, H. Ramlov, P. Hojrup, S. A. Pedersen, L. Hagen, and K. E. Zachariassen, *Insect Biochem. Mol. Biol.* **41**, 109 (2011).
- <sup>16</sup>E. Kristiansen, C. Wilkens, B. Vincents, D. Friis, A. B. Lorentzen, H. Jenssen, A. Lobner-Olesen, and H. Ramlov, *J. Insect Physiol.* **58**, 1502 (2012).
- <sup>17</sup>A. Hakim, J. B. Nguyen, K. Basu, D. F. Zhu, D. Thakrai, P. L. Davies, F. J. Isaacs, Y. Modis, and W. Meng, *J. Biol. Chem.* **288**, 12295 (2013).
- <sup>18</sup>Y. C. Liou, A. Tocilj, P. L. Davies, and Z. Jia, *Nature* **406**, 322 (2000).
- <sup>19</sup>S. Strazdaite, K. Meister, and H. J. Bakker, *Phys. Chem. Chem. Phys.* **18**, 7414 (2016).
- <sup>20</sup>S. Nihonyanagi, S. Yamaguchi, and T. Tahara, *J. Chem. Phys.* **130**, 204704 (2009).
- <sup>21</sup>S. Devineau, K. Inoue, R. Kusaka, S. Urashima, S. Nihonyanagi, D. Baigl, A. Tsuneshige, and T. Tahara, *Phys. Chem. Chem. Phys.* **19**, 10292 (2017).
- <sup>22</sup>K. Meister, S. Strazdaite, A. L. DeVries, S. Lotze, L. L. C. Olijve, I. K. Voets, and H. J. Bakker, *Proc. Natl. Acad. Sci. U. S. A.* **111**, 17732 (2014).
- <sup>23</sup>Y. Otsuki, T. Sugimoto, T. Ishiyama, A. Morita, K. Watanabe, and Y. Matsumoto, *Phys. Rev. B* **96**, 115405 (2017).
- <sup>24</sup>K. Meister, S. Lotze, L. L. C. Olijve, A. L. DeVries, J. G. Duman, I. K. Voets, and H. J. Bakker, *J. Phys. Chem. Lett.* **6**, 1162 (2015).
- <sup>25</sup>J. A. Raymond and A. L. DeVries, *Proc. Natl. Acad. Sci. U. S. A.* **74**, 2589 (1977).